Applied Microbiology and Biotechnology (2019) 103:1877–1891
https://doi.org/10.1007/s00253-018-09585-y

APPLIED MICROBIAL AND CELL PHYSIOLOGY

Impaired oxidative stress and sulfur assimilation contribute to acid tolerance of *Corynebacterium glutamicum*

Ning Xu[1] · Hongfang Lv[2] · Liang Wei[1] · Yuan Liang[1] · Jiansong Ju[2] · Jun Liu[1,3] · Yanhe Ma[1]

Received: 27 August 2018 / Revised: 10 December 2018 / Accepted: 12 December 2018 / Published online: 4 January 2019

Abstract

The industrial organism *Corynebacterium glutamicum* is often subjected to acid stress during large-scale fermentation for the production of bio-based chemicals. The capacity of the cells to thrive in acidic environments is a prerequisite for achieving high product yields. In this study, we obtained an acid-adapted strain using an adaptive laboratory evolution strategy. Physiological characterizations revealed that the adapted strain achieved improved cell viability after acid-stress challenge, with a higher cytoplasmic pH_{in} level, a lower intracellular reactive oxygen species (ROS), and an enhanced morphological integrity of the cells, when compared to those of the original control strain. Transcriptome analysis indicated that several important cellular processes were altered in the adapted strain, including sulfur metabolism, iron transport, and central metabolic pathways. Further research displayed that KatA and Dps cooperatively mediated intracellular ROS scavenging, which was required for resistance to low-pH stress in *C. glutamicum*. Furthermore, the repression of sulfur assimilation by the McbR regulator also contributed to the improvement of acid-stress tolerance. Moreover, two copper chaperone genes *cg1328* and *cg3292* were found to be involved in promoting cell survival under acid-stress conditions. Finally, a new recombinant *C. glutamicum* strain with enhanced acid tolerance was generated by the combined overexpression of *katA*, *dps*, *mcbR*, and *cg1328*, showing 18.4 ± 2.5% higher biomass yields than the wild-type strain under acid-stress conditions. These findings will provide new insights into the understanding and genetic improvement of acid tolerance in *C. glutamicum*.

Keywords *C. glutamicum* · Adaptive laboratory evolution · Acid resistance · Oxidative stress · Sulfur assimilation

Introduction

Bacteria often suffer from diverse external stresses both in natural and industrial environments, such as variations in pH, salinity, temperature, and osmolality (Beales 2004; Marles-Wright and Lewis 2007). Among them, low-pH fluctuations are the most frequent environmental stresses when industrial microorganisms produce acidic bio-based chemicals by fermentation (Liu et al. 2015). Acid stress usually causes a series of physiological damages in the bacterial cells; destroys the structure of biological macromolecules such as nucleic acids, proteins, and lipids; and affects the activities of enzymes involved in major metabolic pathways, thereby leading to the disturbances of intracellular substance/energy metabolism. In order to survive in an unfavorable low-pH environment, bacteria gradually develop a variety of coping strategies during the natural evolution (Kanjee and Houry 2013; Krulwich et al. 2011; Lund et al. 2014; Papadimitriou et al. 2016), such as pumping protons (H^+) out of the cell, producing alkaline substances, synthesizing compatible solutes, altering intracellular redox homeostasis, changing the fatty acid composition of cell membrane, and reconstructing central metabolic pathways.

Ning Xu and Hongfang Lv contributed equally to this work.

Electronic supplementary material The online version of this article (https://doi.org/10.1007/s00253-018-09585-y) contains supplementary material, which is available to authorized users.

✉ Jun Liu
liu_jun@tib.cas.cn

[1] Tianjin Institute of Industrial Biotechnology, Chinese Academy of Sciences, 32 Xiqi Road, Tianjin Airport Economic Area 300308, People's Republic of China

[2] College of Life Sciences, Hebei Normal University, Shijiazhuang 050024, Hebei, People's Republic of China

[3] Key Laboratory of Systems Microbial Biotechnology, Chinese Academy of Sciences, Tianjin 300308, People's Republic of China

In the course of resisting acid stress, self-regulation of intracellular pH levels plays a crucial role in cell survival of microorganisms (Kobayashi et al. 2000). In neutrophilic bacteria, the intracellular pH still maintains a near-neutral state even if the external pH fluctuates within a certain range (Lund et al. 2014). Previous studies have shown that most bacteria employ multiple adaptation strategies to maintain intracellular pH homeostasis, typically by consuming excess protons or producing ammonia through several pathways, such as the glutamate decarboxylase (GAD) system, the arginine deiminase (ADI) system, urea hydrolysis, and F_1F_0-ATPase (Foster 2004; Kakinuma 1998; Kanjee and Houry 2013; Marles-Wright and Lewis 2007; Wu et al. 2014). In most bacteria, for example *Escherichia coli*, *Lactobacillus*, and *Listeria*, the GAD system plays a dominant role in resisting acid stresses, which converts a molecule of glutamate to gamma-aminobutyric acid (GABA) with the removal of an intracellular proton (Lund et al. 2014; Xu et al. 2017).

Corynebacterium glutamicum is generally regarded as a safe microorganism and is widely used for the large-scale fermentation of L-glutamate and various organic acids (Lee et al. 2016; Wieschalka et al. 2013). Interestingly, whole-genome analysis reveals that *C. glutamicum* has no genes with apparent homology to the described GAD and ADI systems (Heydari et al. 2014). In recent years, many studies have revealed that some physiological and biochemical processes are implicated in the defense mechanisms against low pH in *C. glutamicum* (Follmann et al. 2009; Liu et al. 2016; Wang et al. 2016). For example, the comprehensive analysis of pH homeostasis in *C. glutamicum* reveals a functional link among pH response, oxidative stress, iron homeostasis, and metabolic alternations. Mycothiol is a major thiol in most actinomycetes, and it plays an important role in protecting *C. glutamicum* against acid stress by scavenging intracellular reactive oxygen species (ROS). However, the molecular basis of low-pH adaptation in *C. glutamicum* still remains to be described in detail. In this study, an adapted *C. glutamicum* strain showing higher growth capacity at pH 5.6 was obtained by the adaptive laboratory evolution method. According to transcriptome analysis and functional testing, we found that multiple genes implicated in oxidative stress and sulfur assimilation were required for optimal protection against acid stress, providing new candidate functional modules for strain improvement in *C. glutamicum*.

Materials and methods

Strains and growth conditions

Bacterial strains and plasmids used in this study are listed in Table 1. *E. coli* DH5α or HST02 was used as host cells for general cloning. *C. glutamicum* ATCC 13032 was used as the parental strain for gene disruption and the wild-type strain for functional analysis. *E. coli* cells were routinely grown at 37 °C in LB medium (0.5% yeast extract, 1% tryptone, 1% NaCl), and *C. glutamicum* cells were cultivated at 32 °C in modified A medium (designated as the MAM medium) (7 g L^{-1} casamino acids, 5 g L^{-1} $(NH_4)_2SO_4$, 2 g L^{-1} yeast extract, 2 g L^{-1} urea, 0.5 g L^{-1} KH_2PO_4, 0.5 g L^{-1} K_2HPO_4•$3H_2O$, 0.5 g L^{-1} $MgSO_4$•$7H_2O$, 6 mg L^{-1} Fe_2SO_4•$7H_2O$, 4.2 mg L^{-1} Mn_2SO_4•H_2O, 0.2 mg L^{-1} biotin, 0.2 mg L^{-1} thiamine, 4% glucose) unless specified otherwise. When necessary, the medium was buffered with 200 mM MOPS (3-[*N*-morpholino]-propanesulfonic acid, $pK_a = 7.20$), 200 mM MES (2-[*N*-morpholino]-ethanesulfonic acid, $pK_a = 5.96$), or 100 mM homo-PIPES (homopiperazine-1,4-bis[2-ethanesulfonic acid], $pK_a = 4.55$) to different desired pH values, respectively. The pH of each medium was normally adjusted as necessary using either HCl or KOH. If needed, antibiotics were added to a final concentration of 100 μg mL^{-1} ampicillin, 25 μg mL^{-1} kanamycin, or 5 μg mL^{-1} chloramphenicol, and 10 μM isopropyl β-D-1-thiogalactopyranoside (IPTG) was used for the induction of gene expression.

Strain construction

The deletion mutants were achieved by a two-step homologous recombination method based on the temperature-sensitive plasmid pCRD206 as described previously (Okibe et al. 2011). The primers used in this study are listed in Supplemental Table S1. To avoid polar effects, markerless chromosomal in-frame deletion mutants were constructed. The Δ*katA* mutant was obtained as follows: the *katA* upstream and downstream regions were amplified with Phusion High-Fidelity DNA Polymerase using the primer pairs katA-1-For/katA-2-Rev and katA-3-For/katA-4-Rev, respectively. These two products were then fused by overlap extension polymerase chain reaction (OE-PCR) with the primer pairs katA-1-For/katA-4-Rev, ligated into the *Bam*HI/*Xba*I sites of pCRD206, and directly used to transform *E. coli* HST02 to yield the pCRD206-ΔkatA plasmid. The resulting plasmid was then used to transform *C. glutamicum* ATCC 13032 by the electroporation method. The Δ*katA* mutant was obtained through a two-step selection strategy and confirmed by colony-PCR. Similar strategies were used to generate other single-deletion mutants. Moreover, the pCRD206-Δdps plasmid was used to transform *C. glutamicum* Δ*katA* mutant to generate the Δ*katA* Δ*dps* double mutant.

The detailed procedures for the construction of pXMJ19- and pXMJXU-derived recombinant plasmids were described in the Supplemental Methods. The *E. coli-C. glutamicum* shuttle vector pXMJXU, which was obtained by removing the $lacI^q$ region from the pXMJ19 vector (Jakoby et al. 1999), was used as the vector backbone for the improvement of acid-stress tolerance.

Table 1 Plasmids and strains used in this study

Plasmids or strains	Description	Source
Plasmids		
pCRD206	Temperature-sensitive replicon and *B. subtilis sacB* gene, Kan^R	(Okibe et al. 2011
pCRD206-ΔkatA	pCRD206 derivative; contains *C. glutamicum katA* gene flanking region	This study
pCRD206-Δdps	pCRD206 derivative; contains *C. glutamicum dps* gene flanking region	This study
pCRD206-Δftn	pCRD206 derivative; contains *C. glutamicum ftn* gene flanking region	This study
pCRD206-ΔmcbR	pCRD206 derivative; contains *C. glutamicum mcbR* gene flanking region	This study
pXMJ19	*E. coli-C. glutamicum* shuttle vector for IPTG-inducible gene expression, Cm^R	(Jakoby et al. 1999)
pXMJ19-katA	pXMJ19 derivative; carrying *C. glutamicum katA* gene	This study
pXMJ19-dps	pXMJ19 derivative; carrying *C. glutamicum dps* gene	This study
pXMJ19-ftn	pXMJ19 derivative; carrying *C. glutamicum ftn* gene	This study
pXMJ19-katAdps	pXMJ19 derivative; carrying *C. glutamicum katA* and *dps* gene	This study
pXMJ19-mcbR	pXMJ19 derivative; carrying *C. glutamicum mcbR* gene	This study
pXMJXU	pXMJ19 derivative; removing the $lacI^q$ region, Cm^R	This study
pXMJXU-Psod-kd	pXMJXU derivative; carrying *C. glutamicum katA* and *dps* gene under the control of *sod* promoter	This study
pXMJXU-Psod-kdm	pXMJXU derivative; carrying *C. glutamicum katA*, *dps*, and *mcbR* genes under the control of *sod* promoter	This study
pXMJXU-Psod-kdmc	pXMJXU derivative; carrying *C. glutamicum katA*, *dps*, *mcbR*, and *cg1328* genes under the control of *sod* promoter	This study
pXMJXU-Pgap-kd	pXMJXU derivative; carrying *C. glutamicum katA* and *dps* genes under the control of *gap* promoter	This study
pXMJXU-Pgap-kdm	pXMJXU derivative; carrying *C. glutamicum katA*, *dps*, and *mcbR* genes under the control of *gap* promoter	This study
pXMJXU-Pgap-kdmc	pXMJXU derivative; carrying *C. glutamicum katA*, *dps*, *mcbR*, and *cg1328* genes under the control of *gap* promoter	This study
Strains		
DH5α	*E. coli* derivative; competent cells for general cloning	Promega, Madison, WI, USA
HST02	*E. coli* derivative; competent cells for general cloning	Takara, Shiga, Japan
Ori-Cg	Representative wild-type *C. glutamicum* ATCC 13032 strain	Lab stock
Evo-Cg	The improved *C. glutamicum* strain by adaptive laboratory evolution	This study
WT-*katA*	*C. glutamicum* derivative; containing the pXMJ19-katA vector	This study
WT-dps	*C. glutamicum* derivative; containing the pXMJ19-dps vector	This study
WT-*ftn*	*C. glutamicum* derivative; containing the pXMJ19-ftn vector	This study
WT-*katAdps*	*C. glutamicum* derivative; containing the pXMJ19-katAdps vector	This study
WT-*mcbR*	*C. glutamicum* derivative; containing the pXMJ19-mcbR vector	This study
Cg-Psod-kd	*C. glutamicum* derivative; containing the pXMJXU-Psod-kd vector	This study
Cg-Psod-kdm	*C. glutamicum* derivative; containing the pXMJXU-Psod-kdm vector	This study
Cg-Psod-kdmc	*C. glutamicum* derivative; containing the pXMJXU-Psod-kdmc vector	This study
Cg-Pgap-kd	*C. glutamicum* derivative; containing the pXMJXU-Pgap-kd vector	This study
Cg-Pgap-kdm	*C. glutamicum* derivative; containing the pXMJXU-Pgap-kdm vector	This study
Cg-Pgap-kdmc	*C. glutamicum* derivative; containing the pXMJXU-Pgap-kdmc vector	This study

Adaptive laboratory evolution

The adaptive evolution experiment was performed according to the protocols described in the previous literature (Lee et al. 2013). *C. glutamicum* ATCC 13032 was used as the original strain for experimental evolution. The strain was grown aerobically at 32 °C in the 100-mL shake flask containing 20 mL MAM medium, and growth was monitored by measuring the optical density at 600 nm. The MAM medium was buffered with 200 MES to the desired pH values. The medium was sterilized by filtration through a 0.22-μm filter and prepared in sufficient amounts to minimize the possible influences of medium components and pH value. For the adaptive evolution experiment, the cultures were serially passaged at pH 6.0 for the first 25 days and at pH 5.8 for the subsequent 70 days. Every 24 h, the evolving cells were transferred into the

indicated fresh medium to yield an initial optical density (OD_{600}) of 0.1. After finishing the evolution experiment, aliquots of the samples were serially diluted and spread on the MAM plates with a pH of 5.8 to select a single colony of the acid-adapted strain. Dozens of colonies growing faster than the original strain were picked up from the plate and subjected to further evaluation in a liquid medium with an acidic pH of 5.8 (data not shown). Three individual colonies with clearly improved growth were chosen as representatives to test the growth ability of the adapted strain under different acid-stress conditions.

The genetic stability of the adapted strain was also examined after cultivation at normal pH for more than 100 generations. Briefly, the representative colonies of the adapted strain were inoculated into liquid MAM medium with a pH of 7.0 and incubated with shaking at 32 °C. Each cultivation process was started from an initial OD_{600} of 0.1 and was finished with a final OD_{600} of 3.0, resulting in approximately 5 generations. After the adapted strain was transferred a total of 20 times (~ 100 generations), the growth ability of the adapted strain under acid-stress conditions was tested. The growth assay suggested that the adapted strain was genetically stable for many generations (Supplemental Fig. S1).

Transcriptome analysis by RNA-seq

A single colony of *C. glutamicum* original (Ori-Cg) or adapted (Ada-Cg) strains was picked from the freshly streaked agar plate and inoculated into the MAM medium. After overnight cultivation (12–16 h) at 32 °C, the cells were respectively harvested, washed, and shifted to the standard CGXII minimal medium with an initial OD_{600} of 0.1 (Keilhauer et al. 1993). The medium was buffered to pH 5.6 with 200 mM MOPS, and every colony was cultivated in duplicate. The cultures were incubated for a further 12 h at 32 °C before RNA extraction. Total RNA of *C. glutamicum* cells was extracted using the RNAprep Pure Cell/Bacteria Kit (Tiangen Biotech, Beijing, China) and treated with DNase I to eliminate contaminating genomic DNA from the total RNA samples. Library construction and sequencing were performed at Novogene Bioinformatics Technology Co., Ltd. (Beijing, China). The detailed methods for transcriptome analysis are shown in the Supplemental Methods.

Quantitative reverse transcription PCR

Reverse transcription was performed by the RevertAid first-strand cDNA synthesis kit (Thermo Scientific, Waltham, MA, USA) according to the manufacturer's protocol. For the relative qPCR analysis, the reaction mixtures were prepared using SYBR Green Realtime PCR Master Mix (Toyobo Co., Osaka, Japan). The primers used in this procedure are listed in Supplemental Table S2. The experiment was performed in triplicate and repeated three times using an Applied Biosystems 7500 fast real-time PCR system (Thermo Scientific, Waltham, MA, USA). The amplification was performed by an initial denaturation at 95 °C for 1 min, then 40 cycles of 95 °C for 15 s, 60 °C for 15 s, and 72 °C for 40 s, and a final gradient at 55–95 °C for the dissociation curve. The relative gene expression fold changes were calculated according to the delta-delta threshold cycle method after normalization using *16S rRNA* as the internal control (Xu et al. 2018).

Cell growth assay

A single colony from a freshly streaked agar plate was transferred to the liquid MAM medium and incubated for 16 h at 32 °C with shaking at 200 rpm prior to growth experiments. The cultures were harvested, washed, and re-suspended in the fresh indicated medium to an initial OD_{600} of 0.1. Cell growth was then monitored by measuring the optical density at 600 nm at the indicated time points and shown as averages of at least three independent repeats.

Cell survival rate assay

An acid survival assay was carried out according to the previously described method with minor modifications (Zhang et al. 2007). Overnight cultures of *C. glutamicum* were grown to the exponential phase in MAM medium at 32 °C. For strains with IPTG-inducible constructs, 10 μM IPTG was added to the culture medium just 2 h prior to harvesting. The cells were washed with sterile 0.9% NaCl solution and re-suspended in fresh CGXII or 0.9% NaCl solution to an initial OD_{600} of 0.2. These solutions were buffered to pH 4.0 with 100 mM homo-PIPES, unless specified otherwise. The resulting cell suspensions were incubated at 32 °C with shaking of 100 rpm for the indicated time periods. After the low-pH treatment, ten-fold serial dilutions of each sample were spotted onto LBG agar plates (LB medium with 2% glucose) and incubated for 2~3 days before being photographed. Additionally, a 100 μL sample of the 1:10,000 dilution was spread evenly over a fresh LBG plate, and the colonies were counted after 2~3 days of incubation at 32 °C. The survival rates were calculated as the number of colony-forming units (CFUs) after acid challenge divided by the number of CFUs without acid challenge.

Transmission electron microscopy analysis

Cell morphology was examined by TEM analysis as described previously (Wu et al. 2012). Overnight cultures of *C. glutamicum* were pre-grown to the exponential phase in fresh MAM medium. The cells were washed with sterile 0.9% NaCl solution and re-suspended in fresh CGXII medium

buffered to pH 3.8 with 100 mM homo-PIPES. After 2 h of incubation at low pH, the cells were harvested by centrifugation, mixed with 1% low-temp gelling agarose, and further cut into 1-mm^3 dimensioned gel pieces. The samples were prepared according to the standard TEM procedure and observed using an HT7700 transmission electron microscope (Hitachi, Tokyo, Japan).

Measurement of cytoplasmic ROS and pH levels

Cytoplasmic ROS levels were investigated using the fluorescent probe 2′,7′-dichlorodihydrofluorescein diacetate (DCFH-DA) as described previously (Si et al. 2017). Cytoplasmic pH was determined using the pH-sensitive fluorescent probe 2′,7′-bis-(2-carboxyethyl)-5-6-carboxyfluorescein (BCECF) as described previously (Xu et al. 2018). The details of cytoplasmic ROS and pH measurements are shown in Supplemental Methods.

Statistical analysis

Student's *t* test was used to investigate the significance of differences between two groups. Differences with *P* values of less than 0.01 were regarded as statistically significant and were indicated with two asterisks.

Results

Enhancement of acid tolerance in *C. glutamicum* by adaptive evolution

Adaptive laboratory evolution of *C. glutamicum* was performed in two successive stages, with the first 25 days at pH 6.0 and the subsequent 70 days at pH 5.8 (Fig. 1a). Growth assays under variable pH levels revealed that the final acid-adapted clones exhibited obviously enhanced growth compared to the original strain at pH values ranging from 5.2 to 6.0 (Fig. 1b). Growth curve analysis suggested that there was no apparent difference in growth between the original and acid-adapted strains at neutral pH (Supplemental Fig. S2). However, the adapted strain exhibited clearly accelerated growth compared to the original strain when exposed to a more acidic environment of pH 5.6.

The adapted strain showed the improvement of physiological characteristics under acid-stress conditions

In order to further investigate the tolerance of the original and adapted strains to low-pH stress, acid survival assays were examined using ten-fold serial dilutions and CFU counting. As shown in Fig. 2a, with the extension of the incubation period, the survival rates of both strains gradually declined to varying degrees. After 2 h of exposure to the acidic conditions, approximately 39% of the adapted strains remained viable, while the original strain had nearly zero capacity to survive such stress.

To investigate the potential mechanisms underlying these growth differences, the intracellular pH (pH_{in}) and ROS levels were measured by the corresponding fluorescent probes. As shown in Fig. 2b, the adapted strain exhibited higher pH_{in} levels compared to those of the original strain under the lower external pH conditions. For example, the adapted strain maintained a stable pH_{in} of 6.4 against an external pH of 5.5. This value was approximately 0.7 pH units higher than that of the original strain. No obvious difference of pH_{in} was observed between these two strains in a medium with a neutral pH. As expected, Fig. 2c showed that acid stress clearly increased intracellular ROS generation. Under acid-stress conditions, the fluorescence intensity of the adapted strain was approximately 61% of the wild-type level, implying that the adapted strain developed a capacity to reduce the accumulation of intracellular ROS.

The cell wall and membrane of bacteria usually provide the first protective barrier against external stimuli (Silhavy et al. 2010). We therefore used transmission electron microscopy to examine the morphological changes of the original and adapted strains during normal conditions and following acid challenge (Fig. 2d). Under normal pH conditions, both the original and adapted strains had a capacity to maintain the integrity of cell structure, exhibiting a very similar cell wall thickness. By contrast, after 2 h of acid challenge, the cell walls of both strains became thin and their edges were rough. For the original strain, the average thickness of the cell wall was approximately 22.9 nm, and the cells displayed multiple damage sites. However, the cell wall structure of the adapted strain remained relatively intact and smooth, with an average thickness 10.9% greater than that of the original strain. The loss of cell integrity typically led to massive spillage of intracellular materials and severe cytoplasmic vacuolization. In addition, TEM analysis demonstrated that more than 80% of the adapted cells showed elongated phenotype and septum formation, indicating that the adapted strain indeed had enhanced acid tolerance.

Comparative transcriptome analysis revealed candidate genes and key pathways associated with the acid-tolerance phenotype

To further explore the potential molecular mechanisms underlying the improved growth performance of the adapted strain, differential gene expression of the adapted strain compared to the original control under acid-stress conditions was determined by transcriptome analysis. The expression patterns of 212 genes were found to be clearly

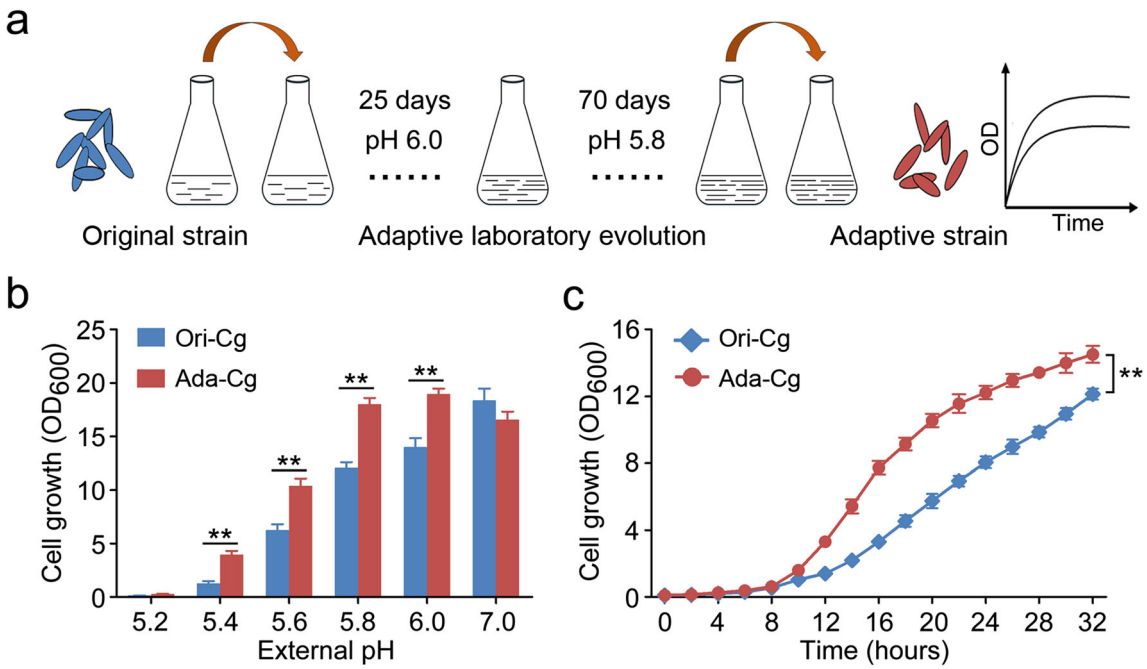

Fig. 1 Adaptive laboratory evolution (ALE) of *C. glutamicum* to improve its acid tolerance. **a** The workflow of the ALE experiment. *C. glutamicum* ATCC 13032 was used as the original strain for experimental evolution. The samples were transferred every 24 h to an initial OD_{600} of 0.1. **b** Growth differences between the original (Ori-Cg) and adapted (Ada-Cg) strains under different pH conditions. Cell growth was determined by measuring the OD_{600} after 20 h of incubation in a shaker at 32 °C. **c** Growth curves of the original and adapted strains in liquid MAM medium at pH 5.6. The data are presented as the means ± standard deviations (SD) from at least three independent experiments. The asterisk indicates a significant correlation between the original and adapted strains at $^{**}P \leq 0.01$

altered at low pH compared with the original strain, including 108 upregulated and 104 downregulated genes (Fig. 3a). Based on KEGG pathway enrichment analysis, these genes were classified into 19 major cellular processes (Fig. 3b and Table 2). Many genes associated with the secondary metabolite biosynthesis, amino acid biosynthesis, carbon metabolism, tricarboxylic acid (TCA) cycle, oxidative phosphorylation, and microbial metabolism diversity were upregulated in the adapted strain. Furthermore, multiple important processes, including sulfur metabolism, biosynthesis of sulfur-containing amino acids, and ATP-binding cassette (ABC) transporters were downregulated in the adapted strain.

Sixteen representative genes were chosen to validate the RNA-seq data by qRT-PCR analysis. As shown in Fig. 3c, the results were in good agreement with the RNA-seq analysis, despite a slight difference in fold changes. Three sulfur assimilation-related genes (*cysD* encoding a sulfate adenylyltransferase, *ssuC* encoding a sulfonate transport system permease protein, and *cysK* encoding a cysteine synthase) as well as two genes of ABC-type transporters (*cg0589* and *cg0768* encoding ATP components of Fe^{3+}-siderophore transport system) were reduced in abundance by at least two-fold, supporting a hypothesis that the adapted strain may have impaired sulfur assimilation or external iron absorption processes. Consistent with this finding, the expression of the *mcbR* gene, encoding a TetR-type transcriptional inhibitor of sulfur metabolism, was approximately 2.6-fold higher in the adapted strain based on the qRT-PCR analysis. Among these upregulated genes, *cg1328* and *cg3292* (encoding copper chaperones) as well as *cg3290* (encoding an oxidoreductase protein) were implicated in copper metabolism and trafficking (Harrison et al. 1999), while *hscA* (encoding a molecular chaperone of the Hsp70/DnaK family) was predicted to maintain cellular protein homeostasis (Genevaux et al. 2007). Moreover, the *cydA* gene (encoding a subunit of cytochrome bd respiratory oxygen reductase) was also upregulated. The enhanced expression of the respiratory bd complex contributes to the extrusion of excess intracellular protons (Giuffre et al. 2014), which was consistent with the higher pH_{in} level displayed by the adapted strain under acid-stress conditions (Fig. 2b). Furthermore, the adapted strain displayed increased expression of *ftsE* (encoding a cell division ATP-binding protein) and *fas* (encoding a fatty acid synthase), which was in agreement with the results of TEM analysis that the adapted strain exhibited improved maintenance of cell division and membrane integrity under acid-stress condition (Fig. 2d) (Letek et al. 2008; Radmacher et al. 2005). Thus, the altered expression of these genes in the adapted strain may also be a non-negligible factor in improving growth performance.

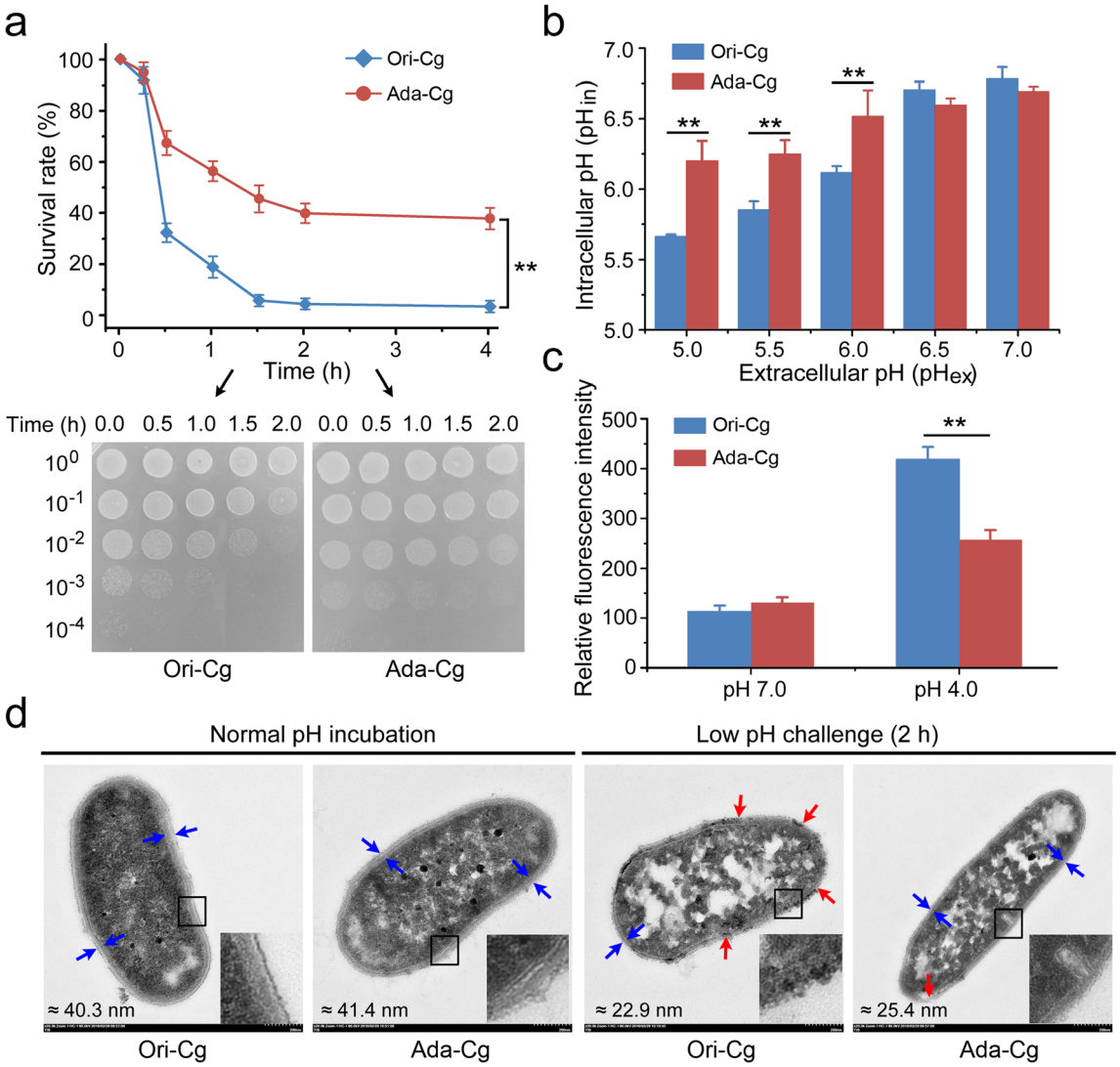

Fig. 2 Differences in physiological properties between the original and adapted strains. **a** Cell survival assays of the two strains after low-pH challenge. After pH 3.8 treatment at the indicated time points, ten-fold serial dilutions were spotted onto LBG agar plates, and colonies were counted after 2~3 days of incubation. **b** Intracellular pH values of the original and adapted strains under various external pH conditions. **c** Cytoplasmic ROS levels of the original and adapted strains at neutral pH 7.0 and acidic pH 4.0. **d** Cell morphology before and after acid challenge was investigated using the transmission electron microscopy. Blue arrows indicate the thickness of the cell wall, and red arrows show possible sites of cell breakage. A 3-times enlarged view of the box was embedded into each image. The asterisk indicates a significant correlation between the original and adapted strains at $^{**}P \leq 0.01$

Scavengers of intracellular ROS were required for the tolerance of *C. glutamicum* to low-pH stress

Previous studies have revealed that acid stress can lead to the formation of intracellular ROS in many microorganisms, including *C. glutamicum* (Chung et al. 2006; Liu et al. 2016; Mols et al. 2010). As the dominant component of ROS, hydrogen peroxide (H_2O_2) is spontaneously converted to the highly reactive hydroxyl radical (OH•) via the Fenton reaction catalyzed by free Fe^{2+} (Winterbourn 1995). These ROS radicals are highly reactive molecules and typically affect cell survival by damaging nucleic acids, lipids, and proteins. The RNA-seq and qRT-PCR data revealed the upregulation of genes associated with intracellular ROS scavenging, such as *katA* encoding a catalase and *dps* encoding a stress-inducible DNA-binding protein (Fig. 3c). Previous studies have demonstrated that Dps can protect DNA from oxidative damage by sequestering intracellular free Fe^{2+} and storing it in the form of an Fe oxyhydroxide mineral (Bellapadrona et al. 2010). Moreover, the expression of the *ftn* gene, encoding a major intracellular iron-storage protein, was obviously upregulated (Rivera 2017). The genes encoding the external Fe^{3+}-siderophore transport system, including *cg0589-0591*,

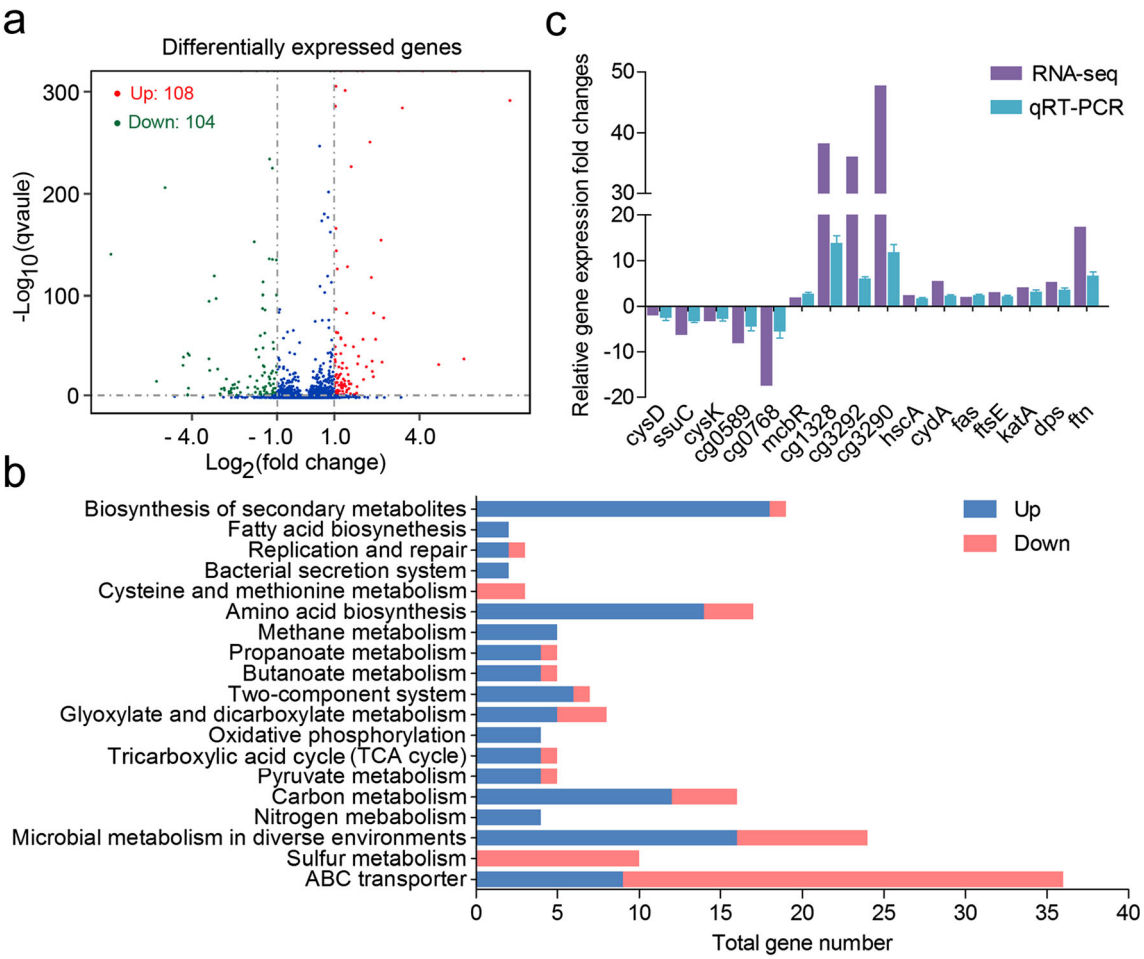

Fig. 3 Transcriptome analysis of the original and adapted strains under acid-stress conditions. **a** Volcano plot of differentially expressed genes. The genes with significant differences were indicated by red (upregulation) and green dots (downregulation). The *X*-axis represents the $\log_2$-transformed value of the expression fold changes, and the *Y*-axis indicates the $\log_{10}$-transformed value of statistically significant differences in expression changes. **b** Expression profiles of genes belonging to different cellular processes according to KEGG analysis. The abscissa represents the number of genes enriched for the indicated metabolic pathways. **c** Relative expression levels of 16 representative genes in the adapted strain compared with those in the original strain identified by RNA-seq and qRT-PCR analyses. The data are presented as the means ± SD from three independent experiments

cg0768-0771, and *cg0924-0928*, were also inhibited in the adapted strain (Table 2). We therefore speculated that the low level of intracellular free Fe^{2+}, largely maintained by both limited external iron uptake and enhanced intracellular iron storage, might be conducive to protecting cells against iron-mediated oxidative stress.

In this study, we selected *katA*, *dps*, and *ftn* as target genes to further investigate their physiological roles in acid tolerance. As shown in Fig. 4a, deletion of *katA* or *dps* significantly reduced the survival rates after low-pH challenge, whereas loss of *ftn* had no apparent effect on the survival of *C. glutamicum* under these conditions. As expected, the overexpression of *katA* or *dps* increased the percentage of viable cells to varying degrees. The double deletion of *katA* and *dps* further exacerbated the survival defect compared to the single-gene deletion, and the Δ*katA* Δ*dps* double mutant showed only 16.6 ± 3.4% survival after low-level acid challenge. Simultaneous overexpression of *katA* and *dps* increased the survival rate to 44.5 ± 3.7%, which was approximately 1.4-fold higher than that of the wild-type strain. The measurement of intracellular ROS levels revealed that they were closely related to the cell survival of different strains (Fig. 4b). The Δ*katA*, Δ*dps*, and Δ*katA* Δ*dps* strains exhibited higher levels of intracellular ROS under acid-stress conditions, which increased by 2.0-, 1.3-, and 2.5-fold compared with the wild-type strain. In accordance with the expectation, overexpression of both *katA* and *dps* led to an obvious reduction of intracellular ROS levels. Taken together, our findings suggest that ROS scavenging mediated by *katA* and *dps* plays an important role in conferring *C. glutamicum* cells with resistance to low-pH stress.

Table 2 Differential gene expression analysis of RNA-seq data between the Evo-Cg and Ori-Cg strain

Gene ID	Name	Annotation	$\log_2$ (fold change)	qvalue
ABC transporters				
cg0405		Cobalamin/Fe^{3+}-siderophore transport system, secreted component	−2.7036	1.49E-06
cg0467		ABC-type cobalamin/Fe^{3+}-siderophore transport system, secreted component	−2.8635	4.12E-08
cg0468		Cobalamin/Fe^{3+}-siderophore transport systems, permease component	−1.5762	0.00062014
cg0469		Cobalamin/Fe^{3+}-siderophore transport system, ATPase component	−2.622	2.64E-05
cg0507		Iron complex transport system permease protein	1.7288	0.0012885
cg0508		Iron/thiamine transport system, secreted component	1.5211	1.43E-09
cg0589		ABC-type iron complex transport system ATP-binding protein	−3.0241	0.00019331
cg0590		Cobalamin/Fe^{3+}-siderophore transport system, permease component	−2.6596	2.77E-06
cg0591		Cobalamin/Fe^{3+}-siderophore transport system, permease component	−2.696	7.43E-05
cg0735	*metI*	D-Methionine transport system permease protein	−1.0707	1.48E-05
cg0736	*metN*	D-Methionine transport system ATP-binding protein	−1.0757	7.61E-10
cg0737	*metQ*	D-Methionine transport system substrate-binding protein	−1.2858	1.57E-136
cg0768		ABC-type cobalamin/Fe^{3+}-siderophore transport system, ATPase component	−4.13	8.45E-10
cg0769		ABC-type cobalamin/Fe^{3+}-siderophore transport system, permease component	−4.3065	2.60E-40
cg0770		ABC-type cobalamin/Fe^{3+}-siderophore transport system, permease component	−4.1014	4.26E-42
cg0771	*irp1*	Iron complex transport system substrate-binding protein	−3.158	7.30E-98
cg0924		Iron complex transport system substrate-binding protein	−3.4045	3.92E-95
cg0926		ABC-type cobalamin/Fe^{3+}-siderophore transport system, permease component	−3.4105	1.08E-38
cg0927		ABC-type cobalamin/Fe^{3+}-siderophore transport system, permease component	−4.1517	7.42E-44
cg0928		ABC-type cobalamin/Fe^{3+}-siderophore transport system, ATPase component	−3.3823	3.25E-27
cg1298	*cydC*	ABC-type multidrug/protein/lipid transport system, ATPase component	2.382	4.26E-21
cg1299	*cydD*	ABC-type multidrug/protein/lipid transport system, ATPase component	2.3455	2.36E-26
cg1418		ABC-type cobalamin/Fe^{3+}-siderophore transport system secreted component	−2.622	1.04E-09
cg2137	*gluB*	Glutamate transport system substrate-binding protein	1.393	5.95E-52
cg2138	*gluC*	Glutamate transport system permease protein	1.4071	9.22E-12
cg2139	*gluD*	Glutamate transport system permease protein	1.1692	9.62E-13
cg2843	*pstB*	ABC-type phosphate transport system, ATPase component	−1.1674	2.97E-07
cg2844	*pstA*	ABC-type phosphate transport system, permease component	−1.784	4.91E-11
cg2845	*pstC*	ABC-type phosphate transport system, permease component	−1.718	3.89E-17
cg2846	*pstS*	ABC-type phosphate transport system, secreted component	−1.0264	2.06E-31
cg3404		ABC-type cobalamin/Fe^{3+}-siderophore transport system, secreted component	−2.5063	1.17E-13
Sulfur metabolism				
cg3253	*mcbR*	TetR-type transcriptional regulator of sulfur metabolism	0.9241	2.17E-07
cg1156	*ssuD2*	Alkanesulfonate monooxygenase	−2.0431	1.62E-10
cg1376	*ssuD1*	Alkanesulfonate monooxygenase	−2.7981	8.59E-19
cg1377	*ssuC*	Sulfonate transport system permease protein	−2.617	6.77E-09
cg1379	*ssuB*	Sulfonate transport system ATP-binding protein	−2.664	1.03E-06
cg1380	*ssuA*	Sulfonate transport system substrate-binding protein	−2.415	3.05E-10
cg2833	*cysK*	Cysteine synthase A	−1.7318	0
cg3114	*cysN*	Sulfate adenylyltransferase subunit 1	−1.0321	1.90E-135
cg3115	*cysD*	Sulfate adenylyltransferase subunit 2	−1.0291	3.08E-101
cg3116	*cysH*	Phosphoadenosine phosphosulfate reductase	−1.1687	4.94E-136
cg3118	*cysI*	Sulfite reductase (ferredoxin)	−1.1143	0
Two-component system				
cg1300	*cydB*	Cytochrome d ubiquinol oxidase subunit II	2.6893	2.01E-35
cg1301	*cydA*	Cytochrome d ubiquinol oxidase subunit I	2.4613	7.61E-58
cg1341	*narI*	Respiratory nitrate reductase gamma subunit	2.6541	5.76E-155
cg1342	*narJ*	Nitrate reductase molybdenum cofactor assembly chaperone	2.0198	7.47E-58

Table 2 (continued)

Gene ID	Name	Annotation	log_2 (fold change)	qvalue
cg1343	*narH*	Nitrate reductase/nitrite oxidoreductase, beta subunit	1.8136	0
cg1344	*narG*	Nitrate reductase/nitrite oxidoreductase, alpha subunit	1.0099	0
Carbon metabolism (including glycolysis and citrate cycle)				
cg0445	*sdhCD*	Succinate dehydrogenase CD	1.06	3.1772E-43
cg0446	*sdhA*	Succinate dehydrogenase A	1.0766	1.7082E-144
cg0791	*pyc*	Pyruvate carboxylase	1.4706	7.85E-129
cg0798	*prpC1*	Citrate synthase	− 1.7718	7.65E-06
cg1451	*serA*	Phosphoglycerate dehydrogenase	1.04	2.7712E-286
cg1726	*mcmA*	Methylmalonyl-CoA mutase	1.1282	2.9925E-64
cg1737	*acn*	Aconitase	2.0026	0
cg2492	*glmS*	Glucosamine-fructose-6-phosphate aminotransferase	1.0194	5.57E-32
cg2559	*aceB*	Malate synthase	− 1.3593	0.00019266
cg2560	*aceA*	Isocitratelyase	− 2.5216	1.29E-09
cg3047	*ackA*	Acetate kinase	2.1338	7.22E-31
cg3048	*pta*	Phosphate acetyltransferase	2.037	2.57E-18
cg3323	*ino1*	Myo-inositol-1-phosphate synthase	1.6787	1.731E-50
Amino acid metabolism				
cg0148	*panC*	Pantoate-β-alanine ligase	1.4503	5.68E-08
cg0149	*panB*	3-Methyl-2-oxobutanoate hydroxymethyltransferase	1.1934	4.05E-07
cg0303	*leuA*	2-Isopropylmalate synthase	1.0293	2.96E-22
cg0755	*metY*	*O*-Acetylhomoserine(thiol)-lyase	− 1.5192	4.56E-88
cg0811	*dtsR2*	Propionyl-CoA carboxylase, beta chain	1.066	2.03E-87
cg1133	*glyA*	Glycine hydroxymethyltransferase	1.2417	0.00E+00
cg1435	*ilvB*	Acetolactate synthase I/II/III large subunit	1.2346	9.61E-44
cg1436	*ilvN*	Acetolactate synthase I/III small subunit	1.5096	9.63E-17
cg1698	*hisG*	ATP phosphoribosyltransferase	1.2261	8.66E-24
cg1726	*mcmA*	Methylmalonyl-CoA mutase	1.1282	2.99E-64
cg2334	*ilvA*	Threonine dehydratase	1.1216	1.83E-19
cg2779	*serB*	Phosphoserine phosphatase	1.0796	4.09E-23
cg2833	*cysK*	*O*-Acetylserine(thiol)-lyase	− 1.7318	0
Copper metabolism				
cg1328		Putative copper chaperone	5.2551	0
cg1329	*ctpC*	Cation transport ATPase	5.2882	0
cg3290		Putative oxidoreductase protein	5.5757	1.68E-38
cg3292		Putative copper chaperone	5.1722	0.00E+00
cg3293		Hypothetical protein predicted by Glimmer/Critica	7.1941	9.28E-292
cg3295		Cation transport ATPase	6.2344	0
cg0569		Probable cation-transporting ATPase	3.2692	0
Other cellular processes				
cg0310	*katA*	Catalase	2.0317	1.79E-59
cg3327	*dps*	Starvation-induced DNA protecting protein, Fe-binding and storage protein	2.3922	1.43E-83
cg2782	*ftn*	Ferritin-like protein	4.1232	0.00E+00
cg0957	*fas*	Fatty acid synthase, bacteria-type fatty acid biosynthesis pathway	1.0609	1.03E-305
cg0914	*ftsE*	Cell division ATP-binding protein	1.1256	3.25E-13
cg0915	*ftsX*	Cell division permease protein	1.5786	2.42E-04
cg3381	*tatA*	Sec-independent protein translocase protein, bacterial secretion system	3.4061	8.40E-285
cg2611	*hscA*	Molecular chaperone, HSP70/DnaK family	1.2805	2.74E-29

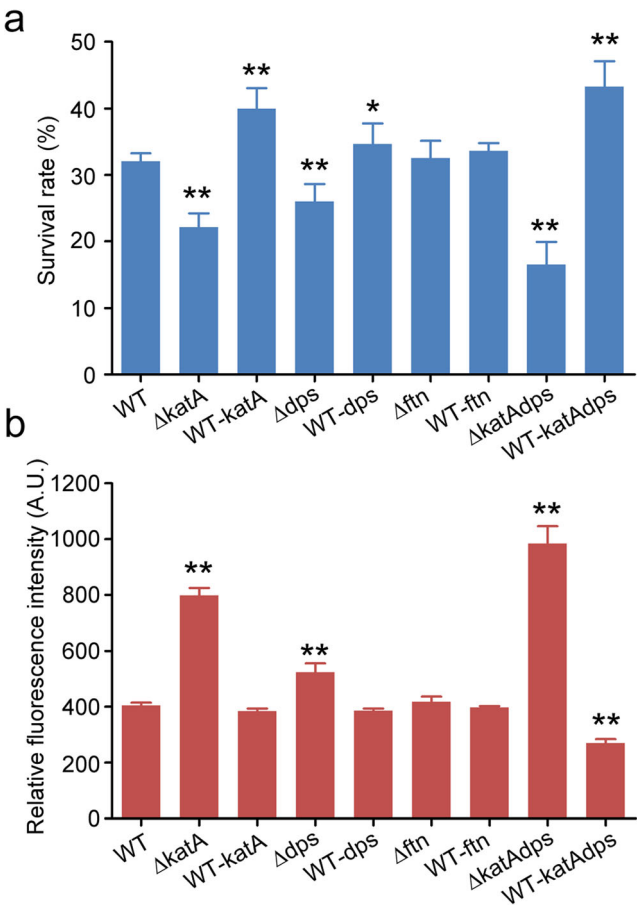

Fig. 4 Effects of *katA*, *dps*, and *ftn* on cell survival and intracellular ROS accumulation. **a** Cell survival assays of the wild-type and mutant strains after low-pH challenge. **b** Cytoplasmic ROS levels of the wild-type and mutant strains after low-pH challenge. The data are presented as the means ± SD from three independent experiments. The asterisk indicates a significant correlation between the wild-type and mutant strains at $*P \leq 0.05$ and $**P \leq 0.01$

The repression of sulfur assimilation pathway using the McbR regulator showed beneficial effects on acid-stress tolerance

The RNA-Seq data revealed that the expression of sulfur assimilation-related genes under acid-stress conditions was greatly reduced in the adapted strain compared with the original strain (Fig. 5a, Table 1). Further qRT-PCR analysis suggested that the absence of the *mcbR* gene, encoding a master repressor of sulfur metabolism in *C. glutamicum* (Rey et al. 2003), obviously increased the expression of sulfur assimilation-related genes (Supplemental Fig. S3). In addition, the expression of the *mcbR* gene in the original and adapted strains was also examined by qRT-PCR analysis. As shown in Fig. 5b, there was no obvious difference in transcript levels between the two strains at neutral pH conditions. However, the adapted strain exhibited clearly higher expression levels of *mcbR* gene compared to the original strain when challenged by low-level acid stress. Furthermore, we performed growth experiments to explore the physiological role of *mcbR* under different pH conditions. Deletion or overexpression of *mcbR* had minor effects on cell growth at neutral pH with or without the addition of cysteine (Supplemental Fig. S4). However, deletion of *mcbR* led to a statistically significant decrease in cell growth under low-pH stress, and overexpression of *mcbR* improved the tolerance of *C. glutamicum* to low pH (Fig. 5c). Interestingly, the presence of cysteine had a largely negative effect on cell growth of all strains at low-pH values. In the *mcbR*-overexpression strain, the addition of cysteine greatly decreased cell growth, supporting the opinion that the accumulation of cysteine or its metabolites is detrimental to cell survival under acid-stress condition. We therefore speculated that the observed increased expression of *mcbR* in the adapted strain repressed sulfur assimilation and cysteine biosynthesis, thereby alleviating the growth defects caused by cysteine accumulation under acid-stress conditions.

Genetic engineering of *C. glutamicum* to improve acid resistance

Based on the described experimental data, *katA*, *dps*, and *mcbR* appeared to be promising genetic modules for strain improvement. Furthermore, we found that two copper chaperone genes, *cg1328* and *cg3292*, were also involved in the promotion of cell survival under acid-stress conditions (Supplemental Fig. S5), which was in agreement with the interplay between acid stress and copper toxicity reported in some bacteria (Djoko et al. 2017; Palumaa 2013). Therefore, we selected four target genes (*katA*, *dps*, *mcbR*, and *cg1328*) as representatives for the construction of strains with enhanced acid tolerance. The functional module designed to confer acid tolerance was overexpressed under the control of the native promoter of *C. glutamicum* superoxide dismutase (*sod*) or glyceraldehyde-3-phosphate dehydrogenase (*gap*). At neutral pH, the overexpression of these potential acid-tolerance modules had slightly negative effects on cell growth during the initial 24 h of incubation, and the engineered strains ultimately showed similar growth phenotypes with the wild-type control (Supplemental Fig. S6). Under acidic conditions, these engineered strains also showed reduced cell growth during the initial incubation period, but their growth rates gradually increased with the extension of incubation (Fig. 6). As expected, the recombinant strain with a combined expression of four target genes under the control of the *gap* promoter reached the highest biomass yield, which was 18.4 ± 2.5% higher than that of the wild-type strain. Overall, this study provides several candidate genetic modules for the improvement of acid tolerance in *C. glutamicum*.

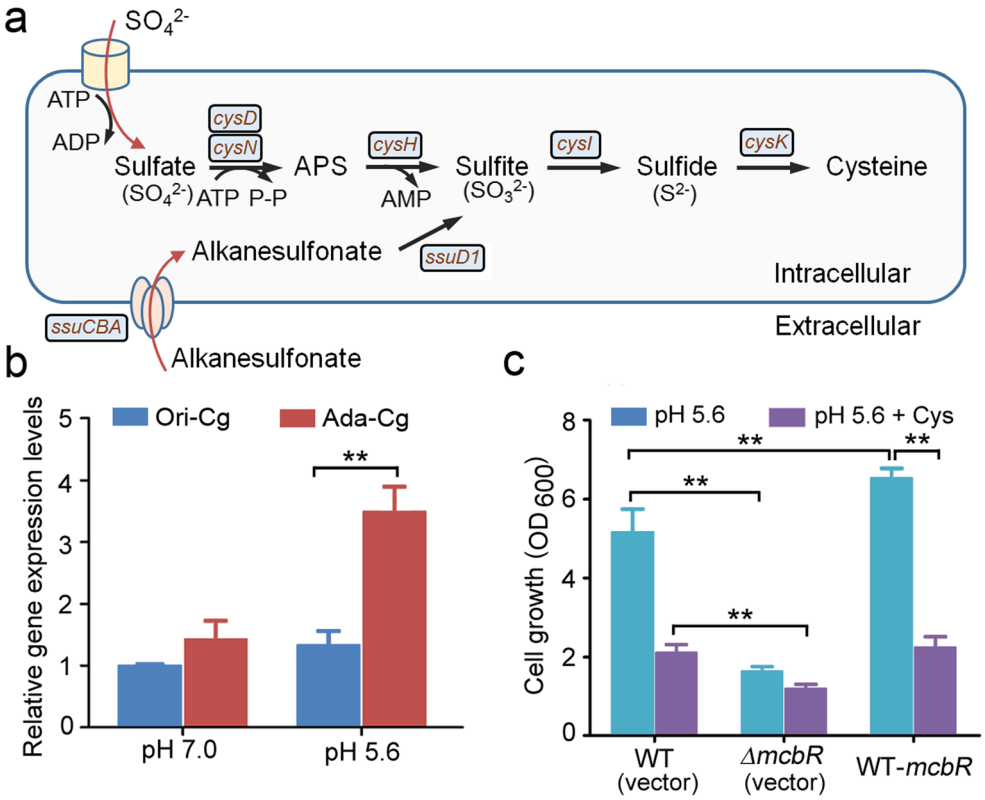

Fig. 5 Roles of the McbR regulator in the response to acid stress. **a** Schematic diagram of the sulfur assimilation pathway in *C. glutamicum*. **b** The mRNA levels of *mcbR* between the original and adapted strains under neutral pH 7.0 and acidic pH 5.6 conditions. **c** Growth differences among the wild-type, Δ*mcbR* deletion, and *mcbR*-overexpression mutant strains under acidic pH conditions with or without 5 mM cysteine. Cell growth was determined by measuring the OD_{600} after 20 h of incubation

Discussion

Acid stress has previously been reported to be associated with oxidative stress in many microorganisms, including *Bacillus cereus*, *E. coli*, and *C. glutamicum* (Lund et al. 2014; Mols et al. 2010; Wang et al. 2016). Here, we found that the adapted strain exhibited reduced intracellular ROS formation under acid-stress condition, and overexpression of both *katA* and *dps* obviously reduced intracellular ROS accumulation and eventually elevated cell survival at acidic pH condition. Previous studies have reported that several regulators, including OxyR, RipA, and DtxR, are involved in the regulation of hydrogen peroxide-inducible antioxidant genes, (Follmann et al. 2009; Heydari et al. 2014). Studies performed in *C. glutamicum* revealed that the LysR-type regulator OxyR acts as a transcriptional repressor of *katA*, *dps*, *ftn*, and *cydA* (encoding a subunit of cytochrome bd oxidase) (Teramoto et al. 2013). The AraC-type regulator RipA also functions as a transcriptional repressor of *katA*, *acn* (encoding an aconitase), and other genes encoding iron-containing proteins,

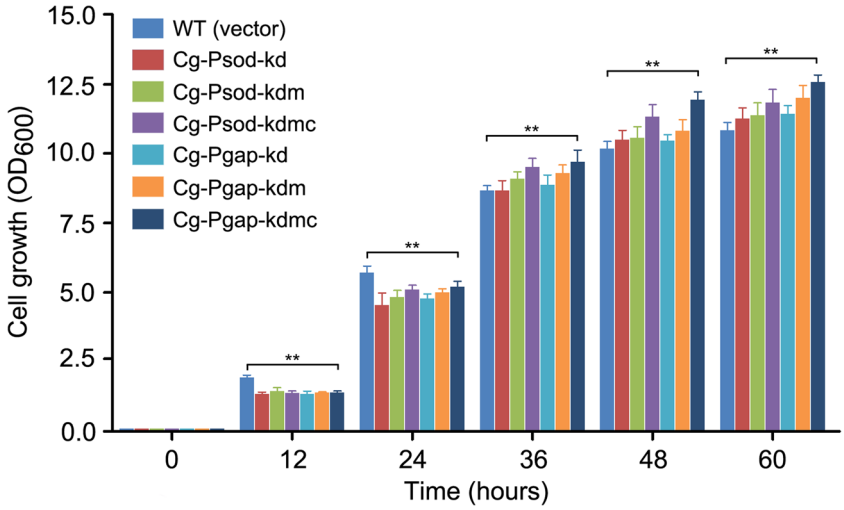

Fig. 6 Growth assays of the wild-type and genetically engineered strains under acid-stress condition. The overnight cultures of the bacterial strains were inoculated into fresh MAM medium with an initial OD_{600} of 0.1. Cell growth was monitored by measuring the optical density at 600 nm at the indicated time points and shown as the averages of three independent repeats. The asterisk indicates a significant correlation between the wild-type and mutant strains at $^{**}P \leq 0.01$

which is itself repressed by the global iron repressor DtxR under iron excess (Wennerhold et al. 2005). The DtxR protein acts as a dual transcriptional regulator to control iron metabolism in *C. glutamicum* and participates in the activation of *ftn* and *dps* (Brune et al. 2006). Interestingly, although our results indicate that the mRNA levels of *katA*, *dps*, *ftn*, *cydA*, and *acn* genes were greatly increased in the adapted strain compared to the original strain under acid-stress conditions, the gene expression of *oxyR*, *ripA*, and *dtxR* showed no obvious changes. One possible explanation for this finding is that these three regulatory genes might be affected at the genomic or protein levels rather than at the transcriptional level. The combined analysis of multi-omics data in future research may contribute to a better understanding of the mechanisms by which *oxyR*, *ripA*, and *dtxR* participate in the incremental expression of most identified antioxidant genes.

Sulfur is an essential macronutrient that is required for the growth of all known living organisms (Rausch and Wachter 2005). However, the accumulation of certain sulfur-containing intermediates, such as cysteine, can disrupt intracellular thiol homeostasis and cause oxidative damage by driving the Fenton reaction (Park and Imlay 2003). The transcriptional repressor McbR has been found to be a master regulator of sulfur assimilation and the biosynthesis of sulfur-containing amino acids in *C. glutamicum* (Rey et al. 2003). In this study, we also found that the expression levels of *mcbR* and sulfur assimilation-related genes were clearly altered in the adapted strain compared to those of the original strain under acid-stress condition. The impairment of the sulfur assimilation pathway exerted beneficial effects on acid tolerance of the adapted strain. In addition, multiple regulators were also reported to control the expression of genes related to sulfur metabolism, such as OxyR and CysR (Milse et al. 2014; Ruckert et al. 2008). Similarly, the expression of these regulatory genes in the adapted strain was not affected at the mRNA level.

Our transcriptome data also revealed that multiple cellular processes, such as iron transport and storage, fatty acid synthesis, copper metabolism, cytochrome bd reaction, and cell division regulation, may also play important roles in acid tolerance. The repression of Fe^{3+}-siderophore transport system aids in the maintenance of a low intracellular free iron content and thereby alleviates the production of hydroxyl radicals via the Fenton reaction catalyzed by free Fe^{2+} (Andrews et al. 2003; Follmann et al. 2009; Winterbourn 1995). The upregulation of the respiratory chain complex II (*sdhA/B/C/D*) and the cytochrome bd oxidase complex (*cydA/B*) can promote the extrusion of intracellular protons (Cecchini 2003; Giuffre et al. 2014). Moreover, the activation of fatty acid synthesis (*fas*) and cell division process (*ftsE/X*) might also be conducive to acid-stress tolerance. However, the detailed mechanisms underlying the roles of these cellular processes need to be deciphered in future research.

Acknowledgements We are grateful to Prof. Masayuki Inui (Research Institute of Innovative Technology for the Earth, Japan) for generously providing plasmids.

Funding This study was supported by the National Natural Science Foundation of China (No. 31500044), the Natural Science Foundation of Tianjin (No. 17JCQNJC09600, No. 17JCYBJC24000), the Tianjin Science and Technology Project (15PTCYSY00020), the Foundation of Hebei Educational Committee (ZD2017047) and the "Hundred Talents Program" of the Chinese Academy of Sciences.

Compliance with ethical standards

Conflict of interest The authors declare that they have no conflict of interest.

Ethical approval This article does not contain any studies with human participants or animals performed by any of the authors.

References

Andrews SC, Robinson AK, Rodríguez-Quiñones F (2003) Bacterial iron homeostasis. FEMS Microbiol Rev 27(2–3):215–237. https://doi.org/10.1016/S0168-6445(03)00055-X

Beales N (2004) Adaptation of microorganisms to cold temperatures, weak acid preservatives, low pH, and osmotic stress: a review. Compr Rev Food Sci F 3(1):1–20. https://doi.org/10.1111/j.1541-4337.2004.tb00057.x

Bellapadrona G, Ardini M, Ceci P, Stefanini S, Chiancone E (2010) Dps proteins prevent Fenton-mediated oxidative damage by trapping hydroxyl radicals within the protein shell. Free Radic Biol Med 48(2):292–297. https://doi.org/10.1016/j.freeradbiomed.2009.10.053

Brune I, Werner H, Huser AT, Kalinowski J, Puhler A, Tauch A (2006) The DtxR protein acting as dual transcriptional regulator directs a global regulatory network involved in iron metabolism of *Corynebacterium glutamicum*. BMC Genomics 7(21):21. https://doi.org/10.1186/1471-2164-7-21

Cecchini G (2003) Function and structure of complex II of the respiratory chain. Annu Rev Biochem 72:77–109. https://doi.org/10.1146/annurev.biochem.72.121801.161700

Chung HJ, Bang W, Drake MA (2006) Stress response of *Escherichia coli*. Compr Rev Food Sci Food Saf 5(3):52–64. https://doi.org/10.1111/j.1541-4337.2006.00002.x

Djoko KY, Phan MD, Peters KM, Walker MJ, Schembri MA, McEwan AG (2017) Interplay between tolerance mechanisms to copper and acid stress in *Escherichia coli*. Proc Natl Acad Sci U S A 114(26):6818–6823. https://doi.org/10.1073/pnas.1620232114

Follmann M, Ochrombel I, Krämer R, Trötschel C, Poetsch A, Rückert C, Hüser A, Persicke M, Seiferling D, Kalinowski J, Marin K (2009) Functional genomics of pH homeostasis in *Corynebacterium glutamicum* revealed novel links between pH response, oxidative stress, iron homeostasis and methionine synthesis. BMC Genomics 10:621. https://doi.org/10.1186/1471-2164-10-621

Foster JW (2004) *Escherichia coli* acid resistance: tales of an amateur acidophile. Nat Rev Microbiol 2(11):898–907. https://doi.org/10.1038/nrmicro1021

Genevaux P, Georgopoulos C, Kelley WL (2007) The Hsp70 chaperone machines of *Escherichia coli*: a paradigm for the repartition of

chaperone functions. Mol Microbiol 66(4):840–857. https://doi.org/10.1111/j.1365-2958.2007.05961.x

Giuffre A, Borisov VB, Arese M, Sarti P, Forte E (2014) Cytochrome bd oxidase and bacterial tolerance to oxidative and nitrosative stress. Biochim Biophys Acta 1837(7):1178–1187. https://doi.org/10.1016/j.bbabio.2014.01.016

Harrison MD, Jones CE, Dameron CT (1999) Copper chaperones: function, structure and copper-binding properties. J Biol Inorg Chem 4(2):145–153. https://doi.org/10.1007/s007750050297

Heydari H, Siow CC, Tan MF, Jakubovics NS, Wee WY, Mutha NV, Wong GJ, Ang MY, Yazdi AH, Choo SW (2014) CoryneBase: *Corynebacterium* genomic resources and analysis tools at your fingertips. PLoS One 9(1):e86318. https://doi.org/10.1371/journal.pone.0086318

Jakoby M, Ngouoto-Nkili CE, Burkovski A (1999) Construction and application of new *Corynebacterium glutamicum* vectors. Biotechnol Tech 13(6):437–441. https://doi.org/10.1023/A:1008968419217

Kakinuma Y (1998) Inorganic cation transport and energy transduction in *Enterococcus hirae* and other *streptococci*. Microbiol Mol Biol Rev 62(4):1021–1045

Kanjee U, Houry WA (2013) Mechanisms of acid resistance in *Escherichia coli*. Annu Rev Microbiol 67:65–81. https://doi.org/10.1146/annurev-micro-092412-155708

Keilhauer C, Eggeling L, Sahm H (1993) Isoleucine synthesis in *Corynebacterium glutamicum*: molecular analysis of the *ilvB-ilvN-ilvC* operon. J Bacteriol 175(17):5595–5603. https://doi.org/10.1128/jb.175.17.5595-5603.1993

Kobayashi H, Saito H, Kakegawa T (2000) Bacterial strategies to inhabit acidic environments. J Gen Appl Microbiol 46(5):235–243. https://doi.org/10.2323/Jgam.46.235

Krulwich TA, Sachs G, Padan E (2011) Molecular aspects of bacterial pH sensing and homeostasis. Nat Rev Microbiol 9(5):330–343. https://doi.org/10.1038/nrmicro2549

Lee JY, Na YA, Kim E, Lee HS, Kim P (2016) The actinobacterium *Corynebacterium glutamicum*, an industrial workhorse. J Microbiol Biotechnol 26(5):807–822. https://doi.org/10.4014/jmb.1601.01053

Lee JY, Seo J, Kim ES, Lee HS, Kim P (2013) Adaptive evolution of *Corynebacterium glutamicum* resistant to oxidative stress and its global gene expression profiling. Biotechnol Lett 35(5):709–717. https://doi.org/10.1007/s10529-012-1135-9

Letek M, Fiuza M, Ordonez E, Villadangos AF, Ramos A, Mateos LM, Gil JA (2008) Cell growth and cell division in the rod-shaped actinomycete *Corynebacterium glutamicum*. Antonie Van Leeuwenhoek 94(1):99–109. https://doi.org/10.1007/s10482-008-9224-4

Liu Y, Yang X, Yin Y, Lin J, Chen C, Pan J, Si M, Shen X (2016) Mycothiol protects *Corynebacterium glutamicum* against acid stress via maintaining intracellular pH homeostasis, scavenging ROS, and S-mycothiolating MetE. J Gen Appl Microbiol 62(3):144–153. https://doi.org/10.2323/jgam.2016.02.001

Liu YP, Tang HZ, Lin ZL, Xu P (2015) Mechanisms of acid tolerance in bacteria and prospects in biotechnology and bioremediation. Biotechnol Adv 33(7):1484–1492. https://doi.org/10.1016/j.biotechadv.2015.06.001

Lund P, Tramonti A, De Biase D (2014) Coping with low pH: molecular strategies in neutralophilic bacteria. FEMS Microbiol Rev 38(6):1091–1125. https://doi.org/10.1111/1574-6976.12076

Marles-Wright J, Lewis RJ (2007) Stress responses of bacteria. Curr Opin Struct Biol 17(6):755–760. https://doi.org/10.1016/j.sbi.2007.08.004

Milse J, Petri K, Ruckert C, Kalinowski J (2014) Transcriptional response of *Corynebacterium glutamicum* ATCC 13032 to hydrogen peroxide stress and characterization of the OxyR regulon. J Biotechnol 190:40–54. https://doi.org/10.1016/j.jbiotec.2014.07.452

Mols M, van Kranenburg R, van Melis CC, Moezelaar R, Abee T (2010) Analysis of acid-stressed *Bacillus cereus* reveals a major oxidative response and inactivation-associated radical formation. Environ Microbiol 12(4):873–885. https://doi.org/10.1111/j.1462-2920.2009.02132.x

Okibe N, Suzuki N, Inui M, Yukawa H (2011) Efficient markerless gene replacement in *Corynebacterium glutamicum* using a new temperature-sensitive plasmid. J Microbiol Meth 85(2):155–163. https://doi.org/10.1016/j.mimet.2011.02.012

Palumaa P (2013) Copper chaperones. The concept of conformational control in the metabolism of copper. FEBS Lett 587(13):1902–1910. https://doi.org/10.1016/j.febslet.2013.05.019

Papadimitriou K, Alegria A, Bron PA, de Angelis M, Gobbetti M, Kleerebezem M, Lemos JA, Linares DM, Ross P, Stanton C, Turroni F, van Sinderen D, Varmanen P, Ventura M, Zuniga M, Tsakalidou E, Kok J (2016) Stress physiology of lactic acid bacteria. Microbiol Mol Biol Rev 80(3):837–890. https://doi.org/10.1128/MMBR.00076-15

Park S, Imlay JA (2003) High levels of intracellular cysteine promote oxidative DNA damage by driving the Fenton reaction. J Bacteriol 185(6):1942–1950. https://doi.org/10.1128/jb.185.6.1942-1950.2003

Radmacher E, Alderwick LJ, Besra GS, Brown AK, Gibson KJ, Sahm H, Eggeling L (2005) Two functional FAS-I type fatty acid synthases in *Corynebacterium glutamicum*. Microbiology 151(Pt 7):2421–2427. https://doi.org/10.1099/mic.0.28012-0

Rausch T, Wachter A (2005) Sulfur metabolism: a versatile platform for launching defence operations. Trends Plant Sci 10(10):503–509. https://doi.org/10.1016/j.tplants.2005.08.006

Rey DA, Pühler A, Kalinowski J (2003) The putative transcriptional repressor McbR, member of the TetR-family, is involved in the regulation of the metabolic network directing the synthesis of sulfur containing amino acids in *Corynebacterium glutamicum*. J Biotechnol 103(1):51–65. https://doi.org/10.1016/S0168-1656(03)00073-7

Rivera M (2017) Bacterioferritin: structure, dynamics, and protein-protein interactions at play in iron storage and mobilization. Acc Chem Res 50(2):331–340. https://doi.org/10.1021/acs.accounts.6b00514

Ruckert C, Milse J, Albersmeier A, Koch DJ, Puhler A, Kalinowski J (2008) The dual transcriptional regulator CysR in *Corynebacterium glutamicum* ATCC 13032 controls a subset of genes of the McbR regulon in response to the availability of sulphide acceptor molecules. BMC Genomics 9:483. https://doi.org/10.1186/1471-2164-9-483

Si M, Zhao C, Burkinshaw B, Zhang B, Wei D, Wang Y, Dong TG, Shen X (2017) Manganese scavenging and oxidative stress response mediated by type VI secretion system in *Burkholderia thailandensis*. Proc Natl Acad Sci U S A 114(11):E2233–E2242. https://doi.org/10.1073/pnas.1614902114

Silhavy TJ, Kahne D, Walker S (2010) The bacterial cell envelope. Cold Spring Harb Perspect Biol 2(5):a000414. https://doi.org/10.1101/cshperspect.a000414

Teramoto H, Inui M, Yukawa H (2013) OxyR acts as a transcriptional repressor of hydrogen peroxide-inducible antioxidant genes in *Corynebacterium glutamicum* R. FEBS J 280(14):3298–3312. https://doi.org/10.1111/febs.12312

Wang T, Gao F, Kang Y, Zhao C, Su T, Li M, Si M, Shen X (2016) Mycothiol peroxidase MPx protects *Corynebacterium glutamicum* against acid stress by scavenging ROS. Biotechnol Lett 38(7):1221–1228. https://doi.org/10.1007/s10529-016-2099-y

Wennerhold J, Krug A, Bott M (2005) The AraC-type regulator RipA represses aconitase and other iron proteins from *Corynebacterium* under iron limitation and is itself repressed by DtxR. J Biol Chem 280(49):40500–40508. https://doi.org/10.1074/jbc.M508693200

Wieschalka S, Blombach B, Bott M, Eikmanns BJ (2013) Bio-based production of organic acids with *Corynebacterium glutamicum*. Microb Biotechnol 6(2):87–102. https://doi.org/10.1111/1751-7915.12013

Winterbourn CC (1995) Toxicity of iron and hydrogen peroxide: the Fenton reaction. Toxico Lett 82-83:969–974. https://doi.org/10.1016/0378-4274(95)03532-X

Wu C, He G, Zhang J (2014) Physiological and proteomic analysis of *Lactobacillus casei* in response to acid adaptation. J Ind Microbiol Biotechnol 41(10):1533–1540. https://doi.org/10.1007/s10295-014-1487-3

Wu C, Zhang J, Wang M, Du G, Chen J (2012) *Lactobacillus casei* combats acid stress by maintaining cell membrane functionality. J Ind Microbiol Biotechnol 39(7):1031–1039. https://doi.org/10.1007/s10295-012-1104-2

Xu N, Wei L, Liu J (2017) Biotechnological advances and perspectives of γ-aminobutyric acid production. World J Microbiol Biot 33(3):64. https://doi.org/10.1007/s11274-017-2234-5

Xu N, Zheng YY, Wang XC, Krulwich TA, Ma YH, Liu J (2018) The lysine 299 residue endows the multisubunit Mrp1 antiporter with dominant roles in Na^+ resistance and pH homeostasis in *Corynebacterium glutamicum*. Appl Environ Microbiol 84(10): e00110–e00118. https://doi.org/10.1128/AEM.00110-18

Zhang J, Fu RY, Hugenholtz J, Li Y, Chen J (2007) Glutathione protects *Lactococcus lactis* against acid stress. Appl Environ Microbiol 73(16):5268–5275. https://doi.org/10.1128/AEM.02787-06